National Conference with International Participation
ENGINEERING MECHANICS 2006
Svratka, Czech Republic, May 15 – 18, 2006
paper no. 254

THREE-DIMENSIONAL ANALYSIS OF RC BEAMS

L. Svoboda [1] **, D. Rypl** [2]

Summary: *The authors are engaged in development of adaptive analysis of RC concrete frames using the microplane model. In this analysis some parts of frame are modelled by 3D finite elements. Therefore several concepts of three-dimmensional analysis of a reinforced concrete beams were tested. Different finite elements and computational schemes were implemented into FEM code and results of numerical verification have been introduced in this work.*

1. Introduction

In this paper the use of the microplane model in an analysis of reinforced concrete beams is discussed. The microplane model is generally a constitutive, fully three-dimensional model capable to describe concrete in its very complex behaviour. Thanks to its qualities, the microplane model is convenient for simulations of experimental results and a comprehensive analysis of various structures from concrete. In particular, the authors have focused on RC frames and have proposed *Adaptive Analysis of RC concrete frames with microplane joints*. It is based on a geometrical model of frame compound of beams and 3D elements (bricks). The microplane model is applied only on bricks, that will be used for segments of the frame with significant nonlinear strains. The rest of the frame will be modelled by beam elements with fibered cross-section, which partly allows simulation of nonlinear behaviour of material.

To get an appropriate three-dimmensional model of RC beam the authors implemented into FEM code a linear 8-node solid element with rotational degrees of freedom. Its advantage against a common linear 8-node solid element is its six degrees of freedom per node. So it can be combined with both truss element (three DOFs per node) and beam element (six DOFs per node). Because the solution time of a commonly used nonlinear static analysis is rather large the authors employed also explicit dynamic relaxation analysis. All above mentioned elements and computational schemes was tested for a fixed-ended beam loaded with mid-span transverse point load.

[1] Ing. Ladislav Svoboda, Czech Technical University in Prague, Faculty of Civil Engineering, Department of Structural Mechanics, Thákurova 7, Prague 6, 166 29, ladislav.svoboda@fsv.cvut.cz
[2] Doc. Dr. Ing. Daniel Rypl, Czech Technical University in Prague, Faculty of Civil Engineering, Department of Structural Mechanics, Thákurova 7, Praha 6, 166 29, drypl@fsv.cvut.cz

2. Microplane Model

The classical constitutive modelling approach is based on a direct relationship between strain and stress tensors and their invariants. Contrary to it, constitutive relations of the microplane model for concrete are formulated in terms of strain and stress components on planes of arbitrary spatial orientation, so-called microplanes. This approach excels in conceptual simplicity and allows straightforward modelling of anisotropy and other features related to planes of different orientation. The penalty to be paid is the great increase of computational effort. Although the microplane theory was originally proposed for plastic behaviour of metals, it can be generally used for any type of material including concrete [Bažant 2000, Caner 2000]. The relationship between micro and macro level is obtained by projecting strain tensor to the particular microplanes (so-called kinematic constraint) or by projecting stress tensor (static constraint). Then constitutive relations between microstrains and corresponding microstresses are evaluated (the constitutive relations can be defined in different ways, depending to it we distinguish four models M1, M2, M3 and M4). The missing link (between micro and macro stresses for kinematic constraint and between micro and macro strain for static constraint, respectively) is obtained by application of the principle of virtual work. Such kind of a material model is capable to describe the triaxial nonlinear behaviour of concrete including tensional and compressive softening, damage of the material, different types of loading, unloading or cyclic loading.

The microplane model is numerically extremely demanding - computation of the stress tensor in a single integration point involves the strain projection to microplanes, the evaluation of local microplane constitutive laws (which may lead to iteration) on each microplane and the homogenization procedure for computing the overall stress tensor. Moreover, the tangent stiffness matrix can be hardly obtained. For some microplane formulations, there is no direct formula and the only possibility is to construct stiffness from its definition. But this is a very expensive procedure. Due to the lack of tangent stiffness one can use the initial elastic matrix for the whole analysis, but this will lead to a very poor convergence. Therefore, the use of implicit methods, which require the stiffness matrix, is cumbersome, due to an extremely slow iteration process.

That is why dynamic relaxation method based on explicit time integration is more efficient. In addition, for nonlinear problems it is convenient to use optimum or quasi-optimum loading minimising inertia forces.

3. Computational Scheme

1. Brief review of the central difference explicit integration method This method is based on the direct integration of the governing equilibrium equation. The equation in time *t* can be written

$$\boldsymbol{M}\ddot{\boldsymbol{r}}_t + \boldsymbol{C}\dot{\boldsymbol{r}}_t + \boldsymbol{F}_t(\boldsymbol{r}_t) = \boldsymbol{R}_t \ , \tag{1}$$

where $\boldsymbol{M}$ and $\boldsymbol{C}$ represent the mass and damping matrices of the discretized system, respectively. $\boldsymbol{R}_t$ is the load vector and $\boldsymbol{F}_t$ is the vector of real internal forces at time *t*. The $\boldsymbol{F}_t$ vector is evaluated using constitutive relations, the microplane model in our case. The new values of displacement, velocities and accelerations at time $t + \Delta t$ are computed from discretized equilibrium equation at time *t* using the known values of displacements $\boldsymbol{r}$, velocities $\dot{\boldsymbol{r}}$ and accelerations $\ddot{\boldsymbol{r}}$ at time *t*. As assumption about the evolution of these characteristics in interval

$\langle t, t+\Delta t\rangle$, a simple differential scheme is used

$$\dot{\boldsymbol{r}}_t = (\boldsymbol{r}_{t-\Delta t} + \boldsymbol{r}_{t-\Delta t})/(2\Delta t) \ , \ \ddot{\boldsymbol{r}}_t = (\boldsymbol{r}_{t+\Delta t} - 2\boldsymbol{r}_t + \boldsymbol{r}_{t-\Delta t})/\Delta t2 \ . \tag{2}$$

Substituting Eqs (2) into Eq. (1) and expressing it in an incremental form, we obtain the following relation

$$\left(\boldsymbol{M}\frac{1}{\Delta t^2} + \boldsymbol{C}\frac{1}{2\Delta t}\right)\Delta r_t = \boldsymbol{R}_t - \boldsymbol{F}_t + \left(\boldsymbol{M}\frac{1}{\Delta t^2} - \boldsymbol{C}\frac{1}{2\Delta t}\right)\Delta \boldsymbol{r}_{t-\Delta t} \ , \tag{3}$$

where $\Delta \boldsymbol{r}_t = \boldsymbol{r}_{t+\Delta t} - \boldsymbol{r}_t$. From this equation, the unknown displacement increment $\Delta \boldsymbol{r}_t$ can be computed. The corresponding vectors of velocities and accelerations can be easily computed using

$$\dot{\boldsymbol{r}}_t = (\Delta \boldsymbol{r}_t + \Delta \boldsymbol{r}_{t-\Delta t})/(2\Delta t) \ , \ \ddot{\boldsymbol{r}}_t = (\Delta \boldsymbol{r}_t - \Delta \boldsymbol{r}_{t-\Delta t})/\Delta t^2 \ . \tag{4}$$

Particularly, the use of diagonal mass matrix $\boldsymbol{M}$ is assumed. If dumping matrix $\boldsymbol{C}$ is expressed in the special form of Rayleigh dumping $\boldsymbol{C} = \alpha\, \boldsymbol{M}$ ($\alpha \in \Re$), one does not need the stiffness matrix. Typically, the nonequilibrated internal forces are applied as loading in the next time step. These choices significantly simplify the solution of the problem and lead to a very efficient computational scheme, which can be parallelized in a straightforward way.

2. Dynamic relaxation using optimum load time history for nonlinear analysis Dynamic relaxation is used in dynamic structural analysis programs based on explicit time integration schemes to make static analysis possible. The solution of the static problem is found as the ultimate settled state of the associated transient dynamic problem. By applying dynamic relaxation we obtain efficient algorithm. Nevertheless, there are drawbacks obstructing the efficient use of this method in nonlinear problems. Conventional dynamic relaxation employs the step function for the load time history. Inertia forces play a significant role in the initial phase of motion before they decay due to damping. In problems involving nonlinear path dependent materials, the final settled state may then differ from the state that would be reached if proportional static loading were applied. Both drawbacks can be eliminated if a slow continuous loading is used instead of the step load, in order to keep the inertia and damping forces small from the very beginning. If a fixed time interval and an ultimate load level are given, the inertia and damping forces depend on the load time history.

Required formula for calculation of the load time history was proposed in [Řeřicha 1986]. Author minimised here the vector of inertia and damping forces

$$\boldsymbol{y}_t = \boldsymbol{M}\ddot{\boldsymbol{r}}_t + \boldsymbol{C}\dot{\boldsymbol{r}}_t = p_t\boldsymbol{P} - \boldsymbol{F}_t \ . \tag{5}$$

This equation follows directly from Eq. (1). The vector $\boldsymbol{P}$ determines the space distribution of the loading (known) and *p(t)* is a time-dependent factor of loading representing wanted load time history. If multi degree of freedom nonlinear undamped systems are considered the following equation is obtained

$$p_t = \frac{1}{\boldsymbol{P}^T\boldsymbol{M}^{-1}\boldsymbol{P}}\boldsymbol{F}_t^T\boldsymbol{M}^{-1}\boldsymbol{P} + c\frac{\tau - t}{\tau} \ , \tag{6}$$

where τ is total time and *c* is a parameter which determines the rate of the loading process and which is evaluated from

$$\boldsymbol{P}^T\boldsymbol{r}_\tau = \frac{c\tau^2}{3}\boldsymbol{P}^T\boldsymbol{M}^{-1}\boldsymbol{P} \ . \tag{7}$$

The vector $\boldsymbol{r}_\tau$ or the scalar $\boldsymbol{P}^T\boldsymbol{r}_\tau$ has to be guessed.

4. Three dimensional 8-node solid element with independent rotation field

In the formulation, first given by Reissner [Reissner 1965], the symmetry of the stress tensor is not enforced "a priori". The skew-symmetric part of the stress tensor appears as a Lagrange multiplier for anforcing the equality of the independent rotation field to the skew-symmetric part of displacement gradient. The variational principle was modified by Hughes and Brezzi [Hughes 1989]. This improved formulation was used as a basis for a new 8-node solid element with independent rotation field first presented by Ibrahimbegovic 1990. In this paper we only present a special hierarchical displacement field employed for the element. For a further details, see the works [Ibrahimbegovic 1991] and [Choi 1996].

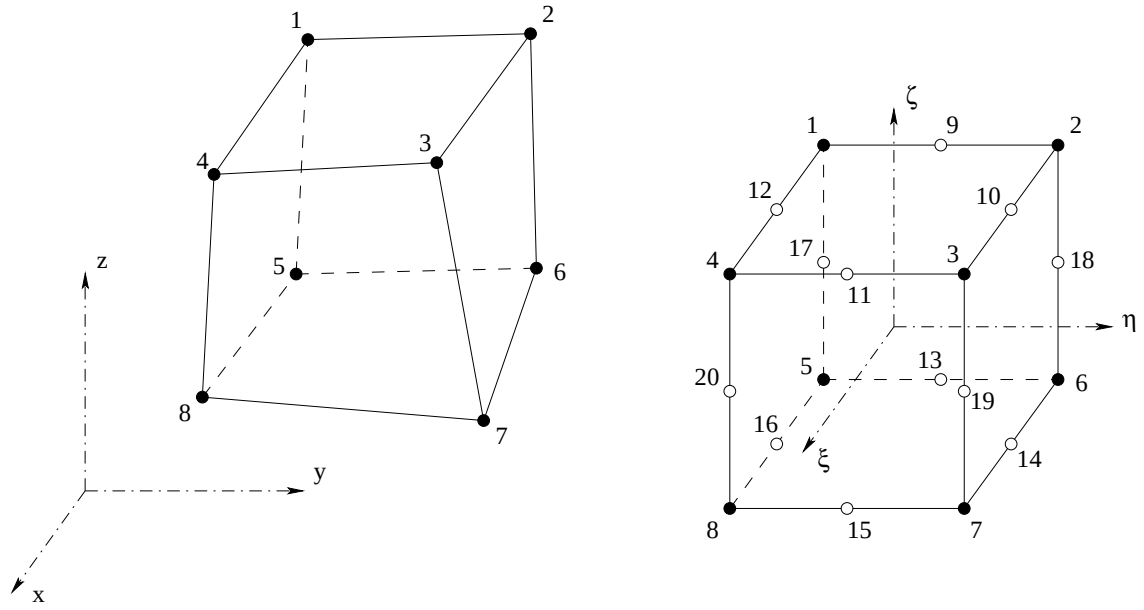

(a) (b)

Figure 1: 8-node solid element with rotational DOFs: (a) in physical coordinate system (b) in natural coordinate system, ● - corner node, ○ - hierarchical mid-edge node.

In the given domain Ω occupied a body, the stress tensor σ is treated as a dependent variable which is assumed as non-symmetric. Additional dependent variables concerned are displacement vector $\boldsymbol{u}$ and a skew-symmetric tensor $\boldsymbol{\psi}$ which represents the rotation. We consider an 8-node solid element shown in Fig. 1. The reference configuration of the element is defined by the 8-node mapping, e.g.

$$\boldsymbol{x}^h = \sum_{I=1}^{8} N_I(\xi,\eta,\zeta)\,\boldsymbol{x}_I \tag{8}$$

where $\boldsymbol{x}^h$ represents global coordinates and N_I are the isoparametric shape functions

$$N_I(\xi,\eta,\zeta) = \tfrac{1}{8}(1+\xi\xi_I)(1+\eta\eta_I)(1+\zeta\zeta_I)\,; \quad I = 1,2,\ldots,8 \tag{9}$$

Natural coordinates (ξ,η,ζ) are defined on the interval $\{-1,1\}$. The non-conventional interpolation for the displacement field $\boldsymbol{u}^h$ of 8-node solid element is derived from a 20-node parent element (see Figs 1 and 2)

$$\boldsymbol{u}^h = \{\, u_1^h\,;\, u_2^h\,;\, u_3^h \,\}^T = \sum_{I=1}^{8} N_I(\xi,\eta,\zeta)\,\boldsymbol{u}_I + \sum_{J=9}^{20} N_J^{edge}(\xi,\eta,\zeta)\,\Delta\boldsymbol{u}_J^{edge} \tag{10}$$

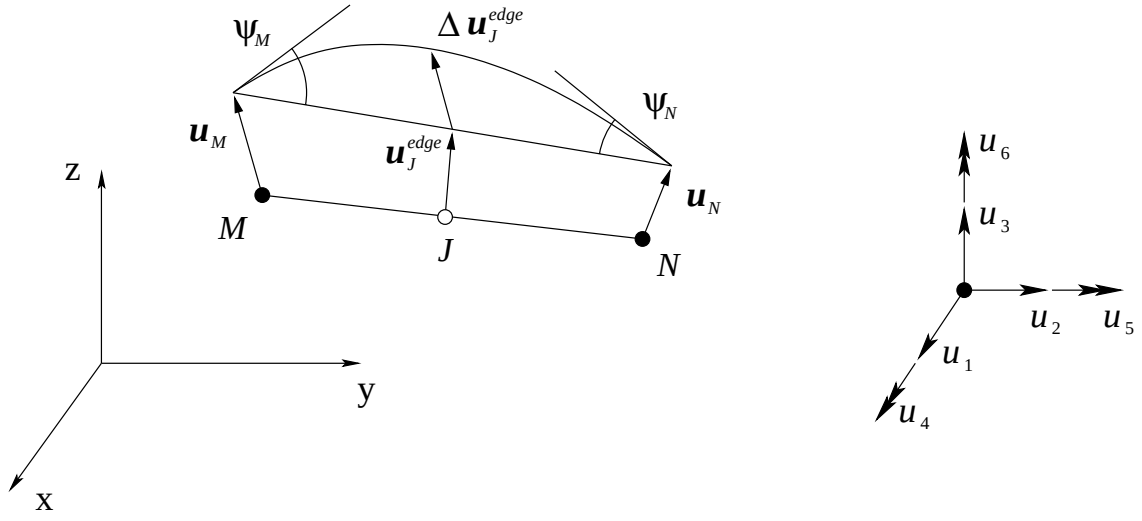

Figure 2: (a) hierarchical interpolation of edge displacement (b) degrees of freedom in a node.

where $\Delta\boldsymbol{u}_J^{edge}$ are twelve hierarchical mid-edge displacement added to the conventional 8-node interpolation values $\boldsymbol{u}_J^{edge} = \frac{1}{2}(\boldsymbol{u}_M + \boldsymbol{u}_N)$ and $N_J^{edge}(\xi,\eta,\zeta)$ are the hierarchical shape functions given as

$$N_J^{edge}(\xi,\eta,\zeta) = \tfrac{1}{4}(1-\xi\xi)(1+\eta\eta_J)(1+\zeta\zeta_J)\,; \quad J = 10,12,16,14 \tag{11}$$

$$N_J^{edge}(\xi,\eta,\zeta) = \tfrac{1}{4}(1+\xi\xi_J)(1-\eta\eta)(1+\zeta\zeta_J)\,; \quad J = 11,15,13,9 \tag{12}$$

$$N_J^{edge}(\xi,\eta,\zeta) = \tfrac{1}{4}(1+\xi\xi_J)(1+\eta\eta_J)(1-\zeta\zeta)\,; \quad J = 19,18,17,20 \tag{13}$$

These hierarchical shape functions are parabolic along the edge joining the adjacent two nodes (see Fig. 2). The mid-edge hierarchical displacement components perpendicular to element edges can be expressed by corner nodal rotations $\boldsymbol{\psi}_M$ and $\boldsymbol{\psi}_N$. This transformation is carried out by the projection of displacement $\Delta\boldsymbol{u}_J^{edge}$ onto xy, xy and xy-plane and can be written as

$$\Delta\boldsymbol{u}_J^{edge} = \boldsymbol{T}_{MN}(\boldsymbol{\psi}_N - \boldsymbol{\psi}_M) \tag{14}$$

$$\boldsymbol{T}_{MN} = \frac{1}{8}\begin{bmatrix} 0 & -l_{MNz} & l_{MNy} \\ l_{MNz} & 0 & -l_{MNx} \\ -l_{MNy} & l_{MNx} & 0 \end{bmatrix} \tag{15}$$

$$\boldsymbol{l}_{MN}^{edge} = \{\, l_{MNx}\,;\, l_{MNy}\,;\, l_{MNz}\,\}^T \tag{16}$$

where $\boldsymbol{l}_{MN}^{edge}$ is a edge vector $\overrightarrow{MN}$.

The resulting element possesses totally 48 degrees of freedom, three displacement components and tree rotations at each of the 8 corner nodes. To minimize the computational cost a 14-point reduced integration was used, see, e.g., [Hoit 1995].

5. Beam for numerical verification

For numerical testing of the above mentioned methods and elements a fixed-ended beam loaded with transverse point load in the middle of the span was used. Bisymmetry of the structure was taken into account to reduce number of finite elements. The reduced FE mesh and the geometry of the whole beam are shown in Fig. 3. The employed constitutive model for concrete was based on microplane model M4. The constitutive properties for brick element of size 30x30x30 mm were following: density ρ = 2500 kg/m^3, dumping coefficient α = 0, Young modulus E = 41039 GPa, Poisson coefficient ν = 0.18, M4 parameters k_1 = 0.000228, k_2 = 500, k_3 = 15, k_4 = 150. Concrete with this parameters approximately corresponds to concrete B50. The beam was reinforced with main and auxiliary longitudinal reinforcement and with stirrups, see Fig. 3. For rods of reinforcement common elasto-plastic material model was used. The yield stress was taken equal to either 600 MPa or infinity (10^6 MPa). The examples were solved with nonlinear static analysis by default.

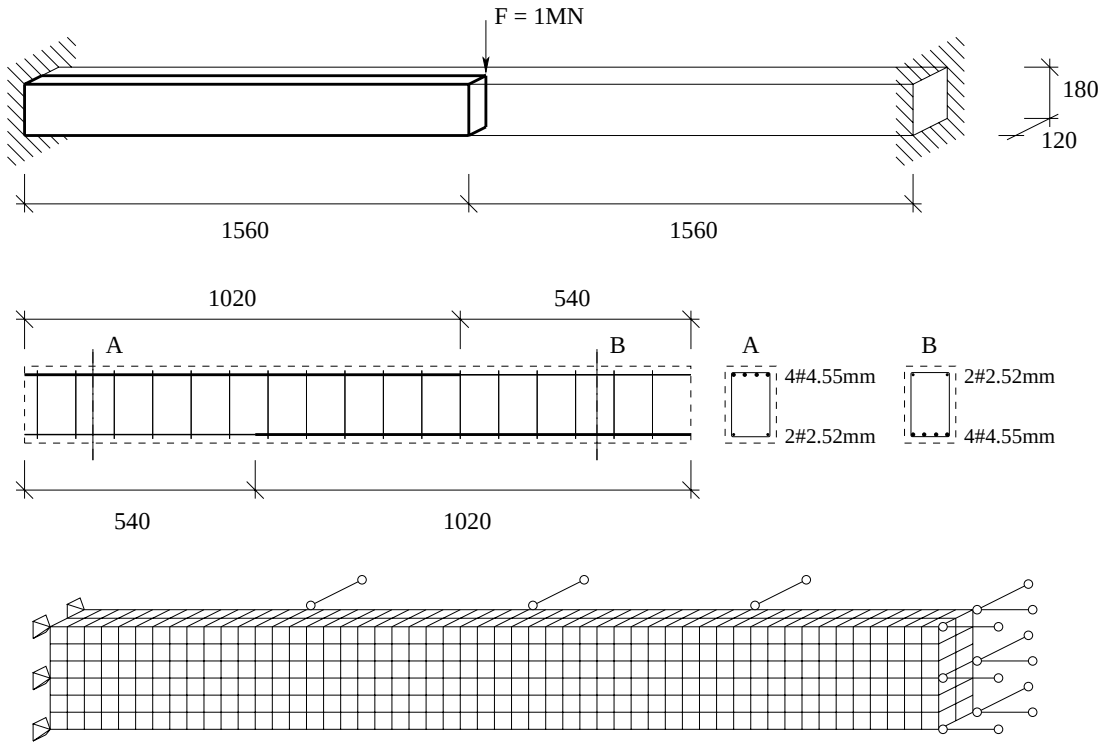

Figure 3: The fixed-ended beam. Geometry of the whole beam, reinforcement of half of the beam and FE mesh of quarter of the beam.

5.1. Influence of reinforcement

At first the influence of stirrups is shown. The test beam was considered with all reinforcement and then without stirrups. Concrete was modelled with linear bricks and reinforcement with truss elements. The yield stress was set to infinity. The comparison of load-deflection curves for both cases of reinforcement is shown in Fig. 4(a). There is a significant point with loadlevel equal to 0.055 in this figure. In the first part of the diagram concrete is nearly elastic in pressure and the stirrups are inactive, both curves are similar. In the second part of the diagram be-

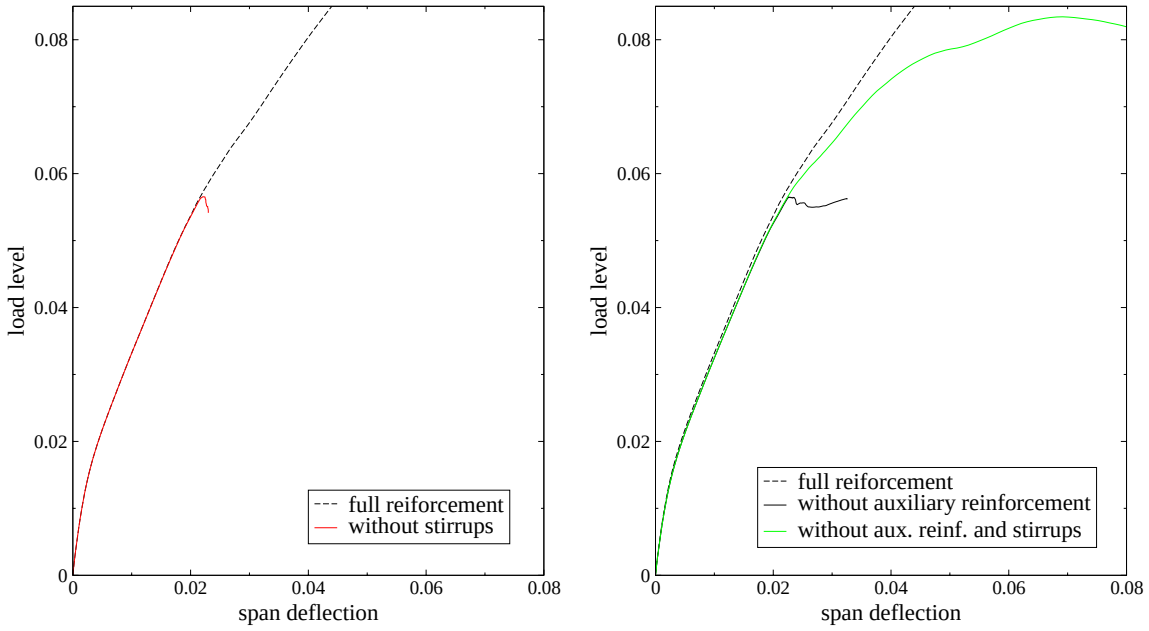

(a) (b)

Figure 4: Load-deflection curves for different reinforcement.

haviour of concrete under pressure and shear is getting significantly nonelastic and the stirrups are activated.

Further the influence of auxiliary longitudinal reinforcement was tested. The load-deflection curves obtained from the beam without konstrukcni reinforcement are similar to previous ones, see Fig. 4(b).

These tests were performed especially to find out the moment of activation of stirrups. In next examples the fully reinforced beam will be supposed.

5.2. Influence of different finite elements

In next examples different finite elements were employed. Common linear bricks and linear bricks with drilling DOFs were used to model concrete. Truss elements and beam elements were used to model rods of reinforcement.

The comparison of brick elements is shown in Fig. 5. Here truss elements were used, the yield stress was set to 600MPa for case (a) and to infinity for case (b). The difference of curves is 2% in the first part of diagram, the diference after activation of stirrups increases approximately to 4%. The solution time of the example with the bricks with rotational DOFs is 2.2 times slower then the second one.

The comparison of truss and beam elements is shown in Fig. 6. Here bricks with rotational DOFs were used because the beam element with six DOFs per node can be combined only with the brick with same number of DOFs per node. The yield stress was set to infinity. The difference of curves after activation of stirrups is approximately 4%.

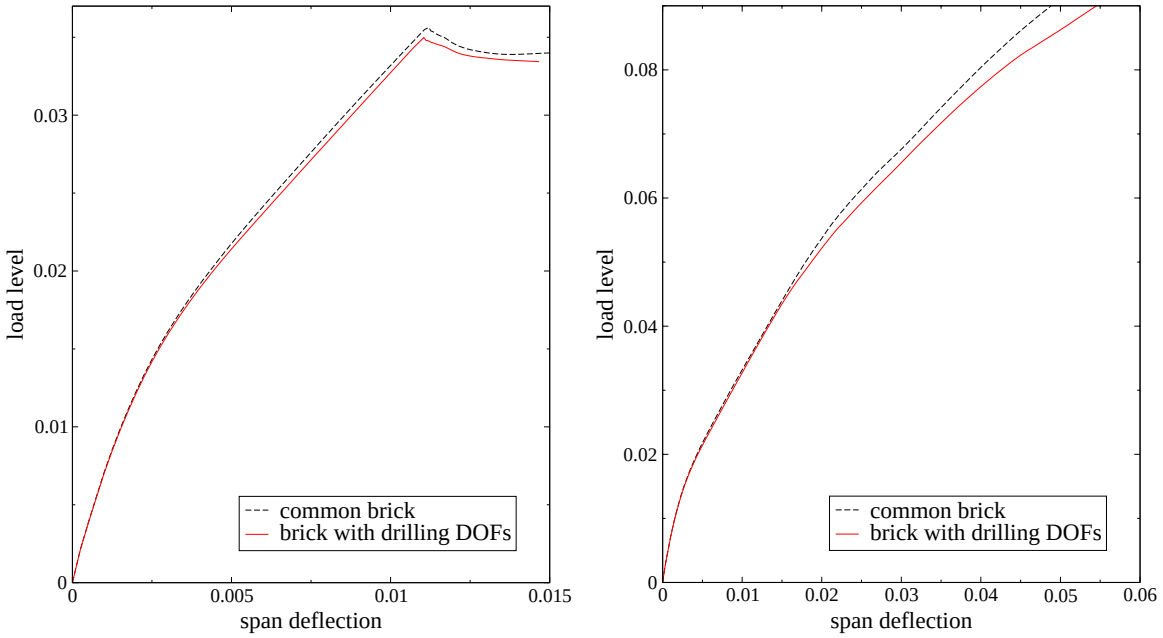

(a) (b)

Figure 5: Load-deflection curves for different brick elements, (a) yield stress is 600MPa, (b) yield stress is infinite.

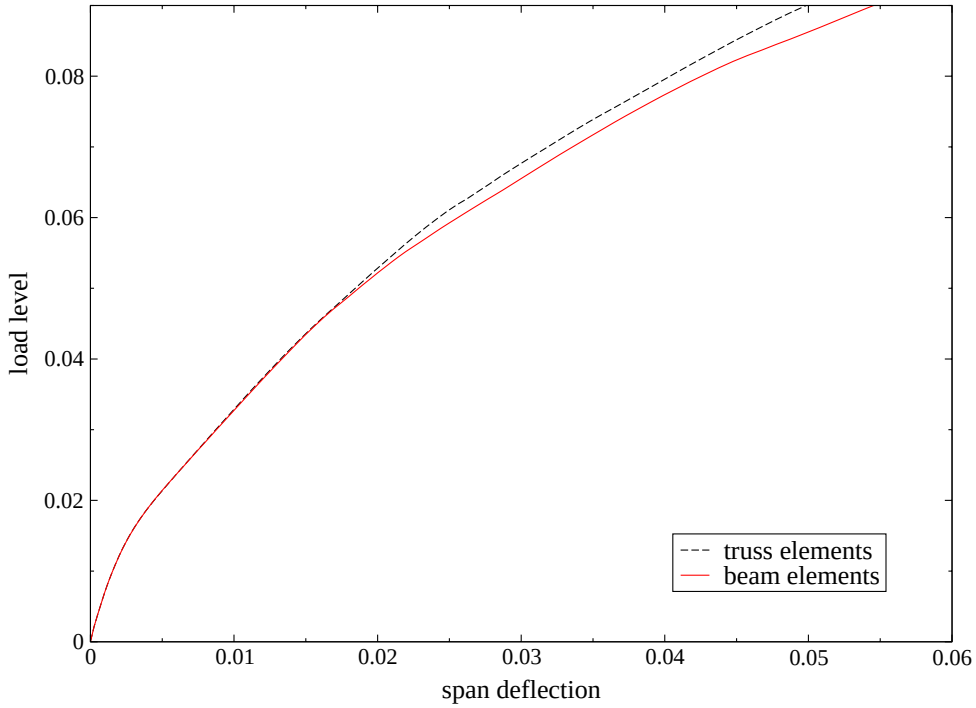

Figure 6: Load-deflection curves for reinforcement rods modelled with different elements.

5.3. Computational schemes

The beam without any reinforcement was solved by both the nonlinear static analysis and the dynamic analysis with dynamic relaxation to compare time consumption, see Fig. 7. It seams

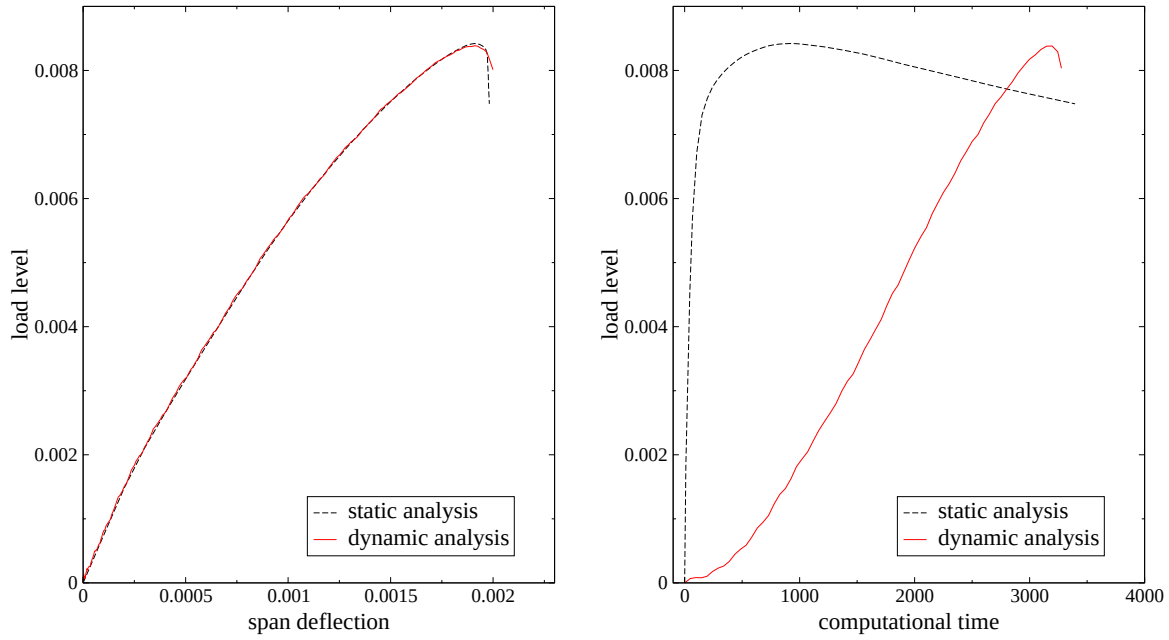

Figure 7: Load-deflection and load-tima curves for different computational schemes.

the total times of both analyses are approximatelly the same. It is true only for this finite element mesh. For increasing number of elements the dynamic analysis becomes faster because this analysis contrary to the static one does not need the stiffness matrix. Further we can see that the static analysis reaches a peak of diagram in a short time but it is very slow after the peak. It is caused by the lack of a tangent stiffness matrix for the microplane model.

To compare accuracy of the analyses the beam with full reinforcement was computed, see Fig. 8. The yield stress was set to 600MPa, see diagram (a), and to infinity, see diagram (b). The obtained load-deflection curves are nearly identical. They differ only in diagram (a) behind the peak since the dynamic relaxation analysis is not able to minimize inertia forces after a sudden reduction of stiffness of a structure.

6. Conclusion

It this paper a three-dimmensional analysis of a reinforced concrete fixed-ended beam was performed. Concrete was modelled by the common linear bricks and by the linear bricks with drilling DOFs. The reinforcement was modelled by truss and beam elements. It appeared that the best result was achieved using the bricks with drilling DOFs combined with beam elements especially in the part of load-deflection diagram after activation of stirrups.

Further the nonlinear static analysis and the dynamic analysis with dynamic relaxation were compared. It seems the static analysis is suitable for FEM models with low number of 3D elements or for research of initial behaviour of beams. The dynamic relaxation analysis is not suitable for structures where quick change of stiffness can occure.

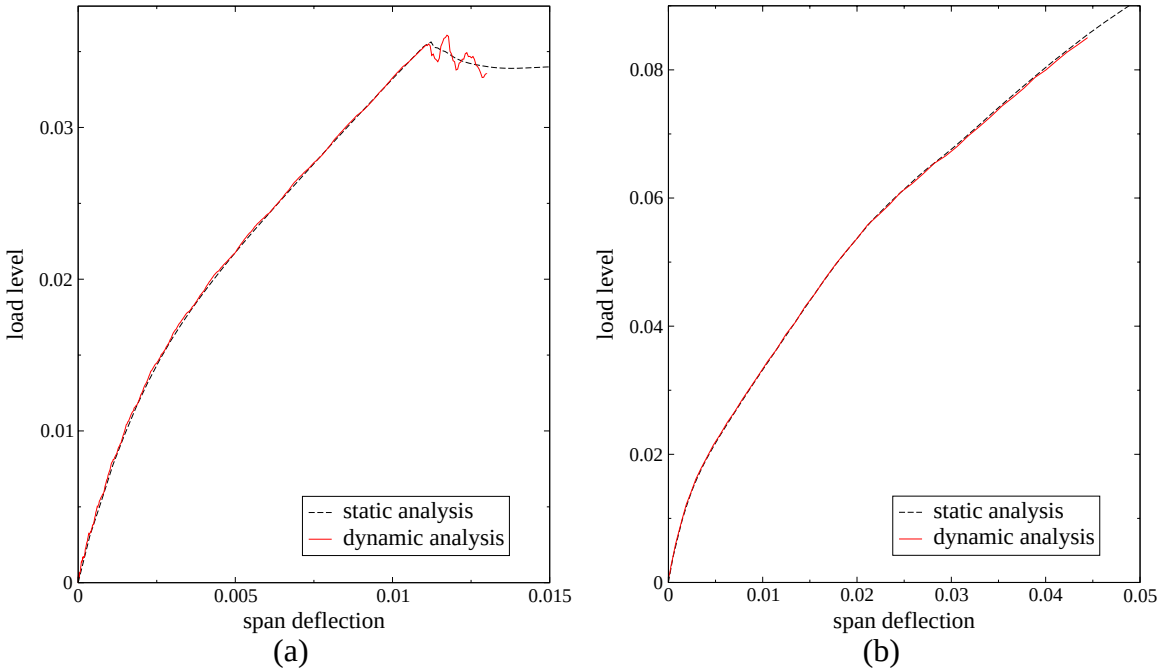

Figure 8: Load-deflection and load-tima curves for different computational schemes.

7. Acknowledgment

The support of the project MSM 6840770003, as well as the project HPC-EUROPA (RII3-CT-2003-506079) and the European Community - Research Infrastructure Action under the FP6 “Structuring the European Research Area” programme is gratefully acknowledged.

8. References

[Bažant 2000] Bažant, Z.P. & Carol, I. & Adley, M.D. & Akers, S.A. 2000: Microplane Model M4 for Concrete I: Formulation with Work-Conjugate Deviatoric Stress. *Journal of Engineering Mechanics*, ASCE 126(9), 944–953.

[Caner 2000] Caner, F.C. & Bažant, Z.P. 2000: Microplane Model M4 for Concrete II: Algorithm and Calibration. *Journal of Engineering Mechanics*, ASCE 126(9), 954–961.

[Řeřicha 1986] Řeřicha, P. 1986: Optimum load time history for non-linear analysis using dynamic relaxation. *International Journal for Numerical Methods in Engineering* 23, 2313–24.

[Reissner 1965] Reissner, E. 1965: A note on variational principles in elasticity. *International Journal of Solids and Structures* 1, 93–95.

[Hughes 1989] Hughes, T.J.R. & Brezzi, F. 1989: On drilling degrees of freedom. *Computer Methods in Applied Mechanics and Engineering* 72, 105–121.

[Choi 1996] Choi, C.K. & Chung, K.Y. & Lee, N.H. 1996: Three dimensional non-conforming 8-node solid elements with rotational degrees of freedom. *Structural Engineering And Mechanics* 4, 569–586.

[Ibrahimbegovic 1991] Ibrahimbegovic, A. & Wilson, E.L. 1991: Thick Shell and Solid Finite Elements with Independent Rotation Fields. *International Journal for Numerical Methods in Engineering* 31, 1393–1414.

[Hoit 1995] Hoit, M.I. & Krishnamurthy, K. 1995: A 14-Point Reduced Integration Scheme for Solid Elements. *Journal of Computers and Structures* 54, 725–730.